Project Title: **Enhanced Power Stability for Proton Conducting Solid Oxides Fuel Cells**
Report Title: **Developing first-principles reactive force fields and densification process for Y-doped $BaZrO_3$ proton-conducting ceramics.**

Type of Report: Semi-Annual Technical Progress Report
Reporting Period Start Date: September 30, 2003
Reporting Period End Date: March 30, 2004

Principle Authors: Boris Merinov, Adri van Duin, Sossina Haile, and William A. Goddard III

Date Report was Issued: April 30, 2004

DOE Award Number: DE-FC26-02NT41631

Name and Address of Submitting Organization: California Institute of Technology, mail code 139-74, 1200 E. California Blvd., Pasadena, CA 91125

DISCLAIMER

ABSTRACT

During the third semi-annual period we have mostly finished a series of QM calculations on relevant metals (Pt, Zr, Y, Ba), metal alloys (Y/Zr), metal oxides (ZrO_2, Y_2O_3, BaO) and Y-doped $BaZrO_3$. Based on these data we started developing ReaxFF for further MD simulations of different physico-chemical processes in the electrolyte and at the electrode/electrolyte interface. To accelerate the densification process of $BaZrO_3$ ceramics at lower temperature an initial screening of all transition elements in the series Sc to Zn has been carried out. It turned out that NiO, CuO and ZnO are the most effective additives for enhancing barium zirconate densification. Characterization (X-ray diffraction, scanning electron microscopy, and impedance spectroscopy) of Zn-, Cu- and Ni-modified BYZ has been performed. The temperature dependence of the bulk conductivity σ_{gi}, grain boundary conductivity σ_{gb}, and specific grain boundary conductivity $\sigma_{sp.gb}$ were measured. The bulk conductivity of BYZ-Zn4 is slightly lower than that of unmodified BYZ.

TABLE OF CONTENTS

LIST OF GRAPHICAL MATERIALS

INTRODUCTION

At present, only electrolytes based on Y-doped $BaZrO_3$ (BYZ) combine high bulk proton conductivity with high chemical and mechanical stability. $BaZrO_3$ belongs to the family of cubic perovskite-type oxides. The high symmetry is essential for the high solubility limit of protonic defects and for the high isotropic proton mobility. The large lattice constant for Y-doped samples and the covalency of the Zr – O bonds reduce the Zr /H repulsive interaction and, therefore, the activation enthalpy of the mobility of protonic defects. Another key feature is the availability of a nearly perfect acceptor dopant. Despite its significantly higher ionic radius compared to Zr^{4+}, $Y^{3+}$is found to be optimal as an acceptor for $BaZrO_3$ [1]. In order to incorporate protons the samples they are exposed to a flow of wet synthetic air at high temperature (~350ºC). Formation of protonic defects can be described as water dissociation into a hydroxide ion and a proton. The hydroxide ion occupy an an oxide ion vacancy and the proton forms a covalent bond with a lattice oxygen:

$$H_2O + V_O^{\bullet\bullet} + O^X{}_O \Leftrightarrow 2OH_O^{\bullet}.$$

Two hydroxide ions substitute for oxide ions and two positively charged protonic defects ($2OH_O^{\bullet}$) are formed. At temperatures about 700ºC BYZ is an excellent high-temperature proton conductor. The observed grain interior proton conductivity clearly exceeds the oxide ion conductivity of the best oxygen conductor, Y-doped ZrO_2. However, the grain-boundary conductivity is significantly lower than the corresponding bulk conductivity. Optimization of grain-boundary properties and processes of preparation of BYZ ceramics could make this material a real alternative for currently used electrolytes in solid oxide fuel cells.

EXECUTIVE SUMMARY

A series of QM calculations of EOS has been performed on various bulk metals (Pt, Zr, Y, Ba), metal alloys (Y/Zr), metal oxides (ZrO_2, Y_2O_3, BaO) and Y-doped $BaZrO_3$ (BYZ). Based on these QM data we have developed ReaxFF for Pt-metal clusters, bulk metals (Pt, Zr, Y, Ba), metal alloys (Y/Zr), metal oxides (ZrO_2, Y_2O_3, BaO) and initial ReaxFF potentials for BYZ. Further development of ReaxFF will allow us to model the structure of the electrolyte, including grain-boundaries, and electrode/electrolyte interface, as well as diffusion and catalytic processes in this type of solid oxide fuel cells. ReaxFF MD simulations could help to find the ways of optimization of the grain-boundary properties. One of them is to increase the density of $BaZrO_3$ ceramics for better contacts between grains. To accelerate the densification process of $BaZrO_3$ ceramics at lower temperature, an initial screening of all transition elements in the series Sc to Zn has been performed. It turned out that NiO, CuO and ZnO are the most effective additives for enhancing barium zirconate densification. The enhanced densification for modified BYZ has been improved to 95%. Characterization (X-ray diffraction, scanning electron microscopy, and impedance spectroscopy) of Zn-, Cu- and Ni-modified BYZ has been performed. The temperature dependence of the bulk conductivity σ_{gi}, grain boundary conductivity σ_{gb}, and specific grain boundary conductivity $\sigma_{sp.gb}$ were measured. The bulk conductivity of BYZ-Zn4 is slightly lower than that of unmodified BYZ.

RESULTS AND DISCUSSION

THEORETICAL

Developing Reactive Force Fields

The accuracy and speed of modern QM methods allow geometries, energies, and vibrational energies to be predicted for small molecules. However, QM is not practical yet for studying the dynamical properties of larger molecules and solids. Therefore, in order to predict important performance characteristics of fuel cell devices it is useful to have force fields that accurately describe chemical reactions, diffusion and other dynamical properties. In general, traditional force fields do not deal in making and breaking bonds, barriers for reactions, etc. Unlike this, ReaxFF [2,3] solely based on *ab initio* QM calculations is especially designed to describe chemical reactivity, dissociation and formation of chemical bonds, surfaces, defects, diffusion, etc. The basic structure of ReaxFF is similar to that employed in many non-reactive force fields in which the system energy is divided up into various partial energy contributions:

$$E_{system} = E_{bond} + E_{over} + E_{under} + E_{lp} + E_{val} + E_{pen} + E_{tors} + E_{conj} + E_{vdWaals} + E_{Coulomb}$$

The fundamental difference is that ReaxFF do not employ the rigid connectivity method to determine the location of chemical bonds but use the bond order method instead. These bond orders, directly calculated from interatomic distances and continuously updated, allow creation and dissociation of bonds during the simulation.

To derive parameters for the ReaxFF training set, we first performed QM-calculations on relevant condensed phases and cluster systems. The calculations were based on Density Functional Theory (DFT) [4,5] using Generalized Gradient Approximation (GGA) [6] to treat the exchange-correlation energy functional. Pseudopotentials were used to replace the core electrons. All calculations were performed at T = 0K. Most of the QM calculations were carried out using the pseudo-potential local basis set code SeqQuest, jointly being developed between Sandia National Laboratories (Dr. Peter Schultz) and Caltech. The obtained QM data were then used to optimize ReaxFF. We currently have the ReaxFF description for Pt-metal clusters[*], various bulk metals (Pt, Zr, Y, Ba), metal alloys (Y/Zr), metal oxides (ZrO_2, Y_2O_3, BaO) and initial parameters for Y-doped $BaZrO_3$.

Bulk metals. For each of the metal atoms in the Y-doped $BaZrO_3$ system and for Y/Zr alloys EOS of several polymorphs were derived from the QM calculations. These data were subsequently used to develop ReaxFF parameters.

Figs.1-4 compare the QM-data to the ReaxFF results. Most weight was given in the ReaxFF parameter optimization to the low-energy phases. For the high-energy phases [i.e. simple cubic (sc)], we gave little weight to the QM EOS but rather focused on making sure that ReaxFF gets the correct energy with respect to the low-energy phases.

[*] ReaxFF description for Pt was presented in the previous semi-annual report.

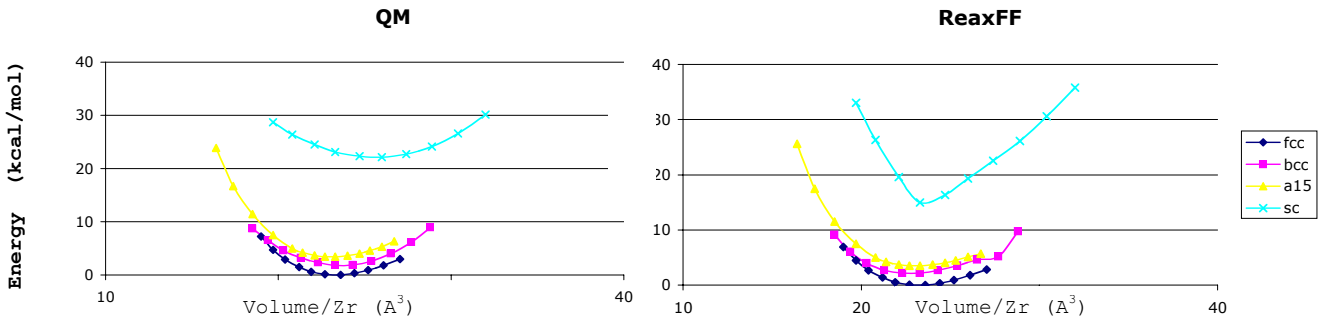

Fig.1. QM- and ReaxFF results for the equation of state of various Zr-polymorphs.

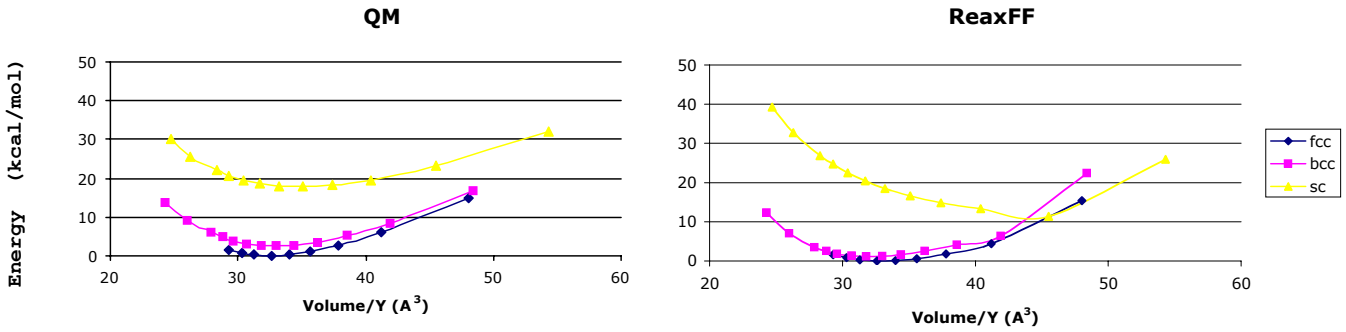

Fig.2. QM- and ReaxFF results for the equation of state of various Y-polymorphs.

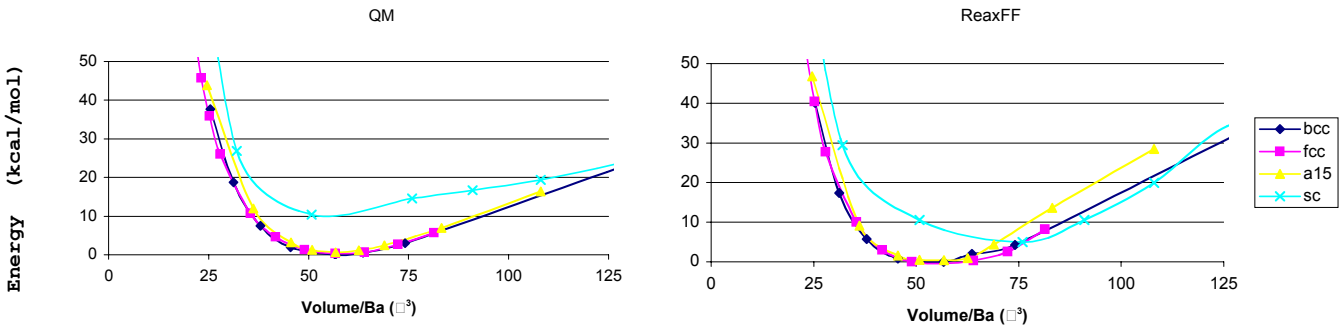

Fig.3. QM- and ReaxFF results for the equations of state of various Ba-polymorphs.

The above Figures demonstrate that ReaxFF provide a good reproduction of the QM EOS and relative energies for the stable metal polymorphs and properly predict the unstable polymorphs to be higher in energy. ReaxFF also predict positive heat of formation for the Y/Zr alloys that indicate that the alloys are less stable than the pure metal phases. Further optimization of the ReaxFF parameters will be performed, in particular, for better description of the EOS of the high-energy simple cubic metal phases.

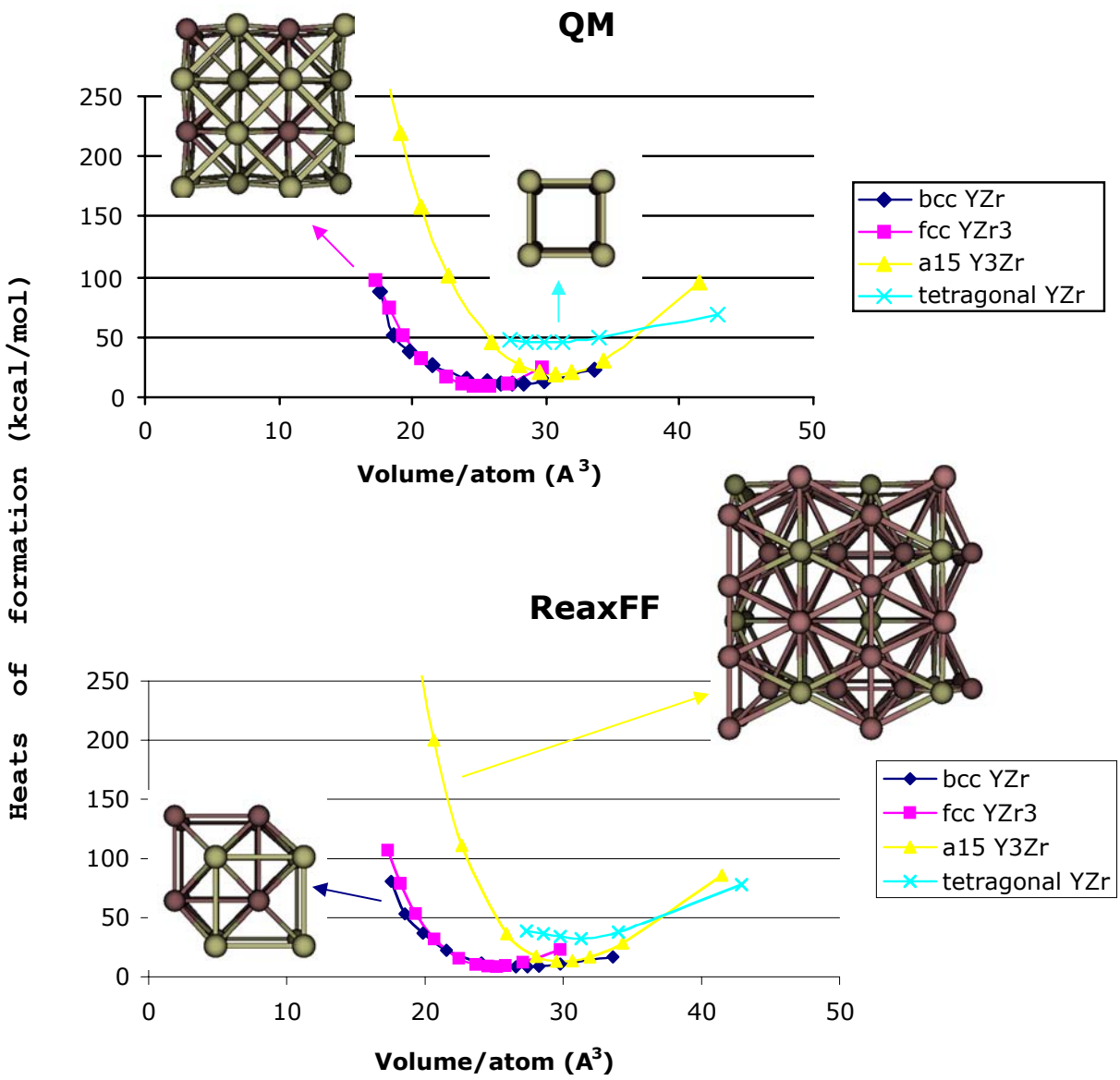

Fig.4. QM- and ReaxFF results for the equations of state of various Y/Zr- alloy polymorphs.

Metal oxides. We also performed a series of QM calculations of EOS on the relevant metal oxides, ZrO_2, Y_2O_3, BaO. ReaxFF should be completely defined in terms of geometry. It means, each metal must be described in different polyhedral environments (tetrahedral, octahedral, cubic etc.). Therefore, ReaxFF need QM data not only for experimentally observed phases but also for some hypothetic phases, for instance, the rutile and BaF_2 phases for ZrO_2, or the corundum phase for Y_2O_3 (see Figures below). Different phases have very different densities and, as it is clearly seen from the Figs.5-7, ReaxFF reproduce all these densities and energies very well.

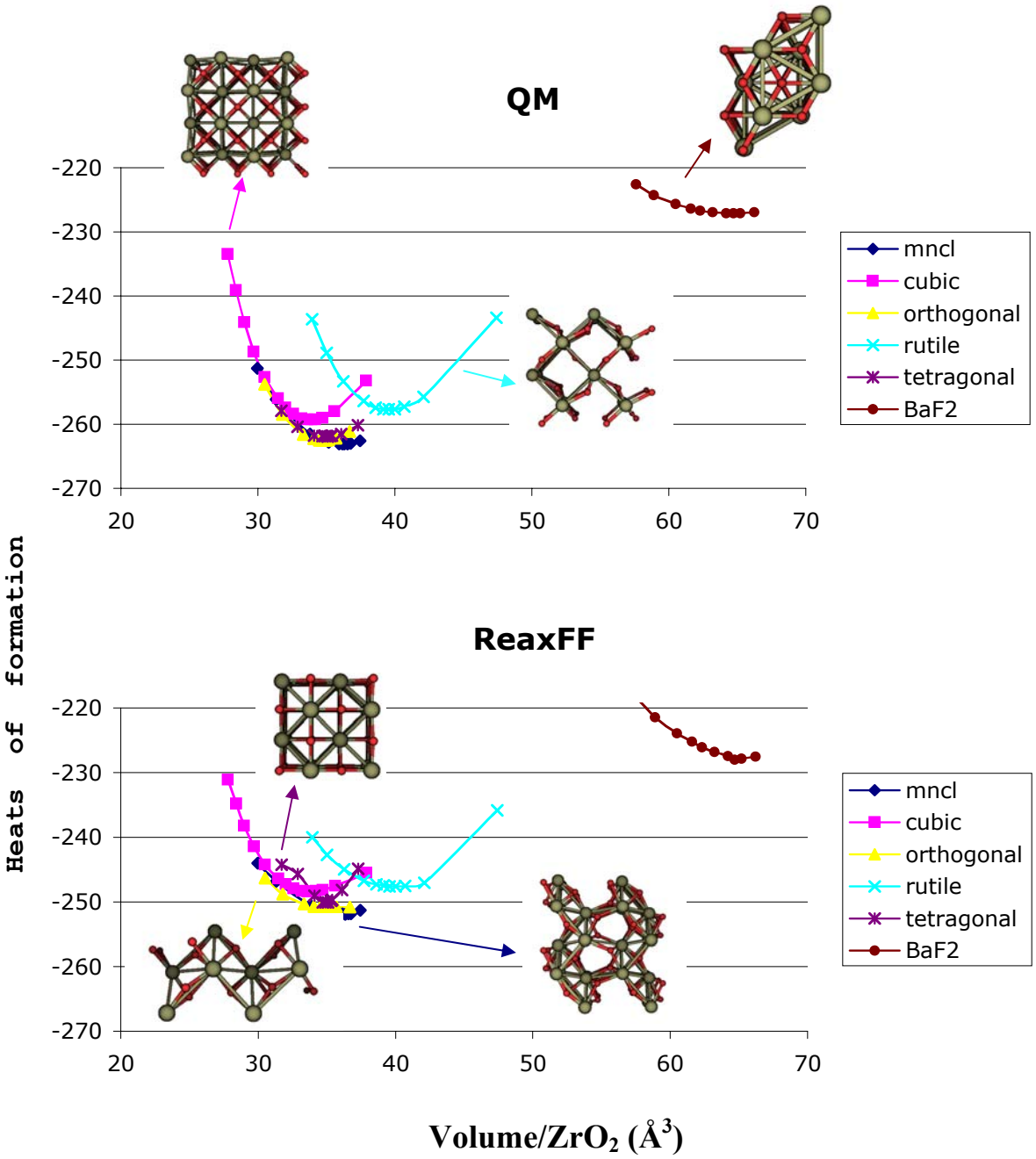

Fig.5. QM- and ReaxFF results for the equations of state of various ZrO_2 polymorphs.

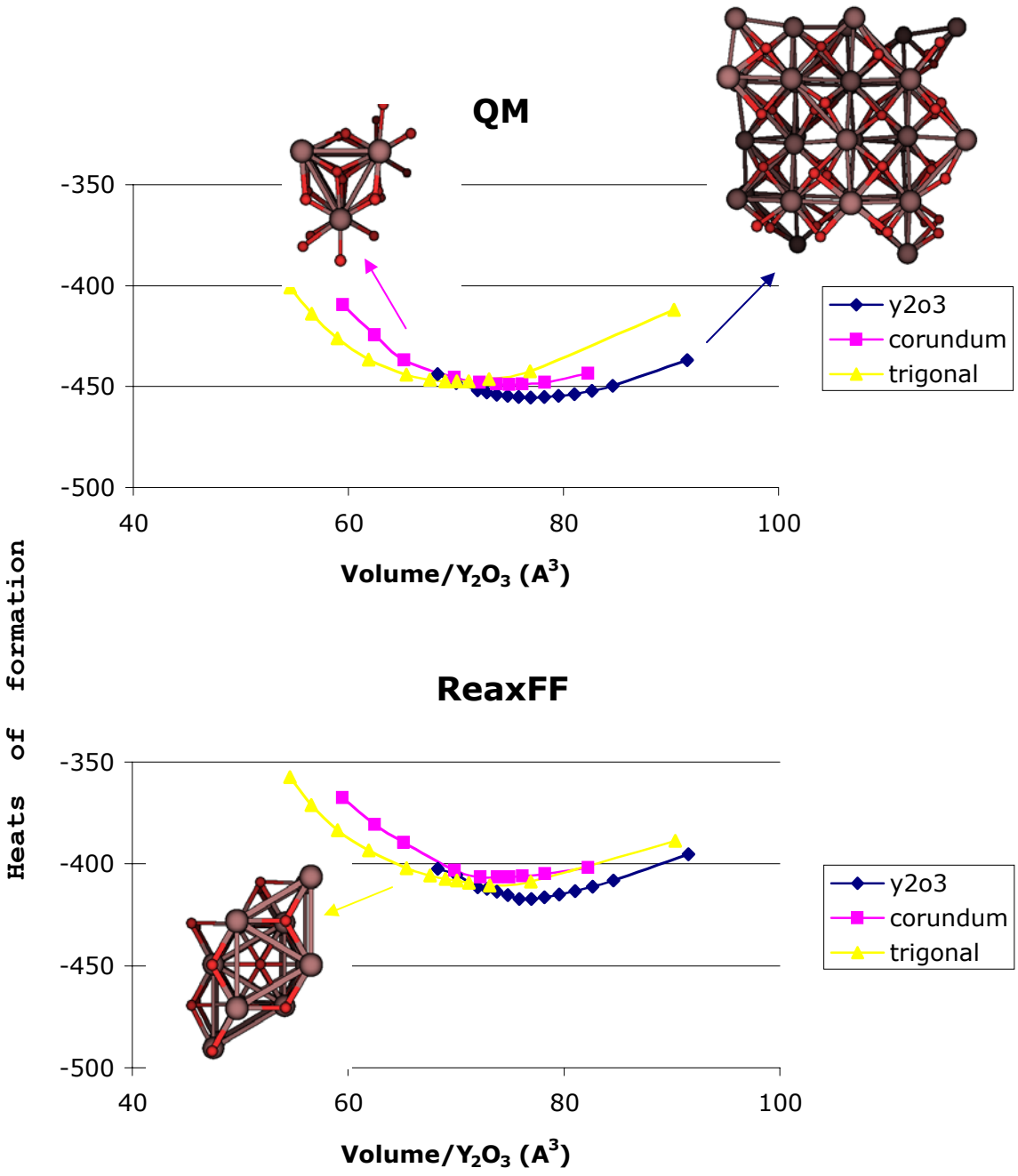

Fig.6. QM- and ReaxFF results for the equations of state of various Y_2O_3 polymorphs.

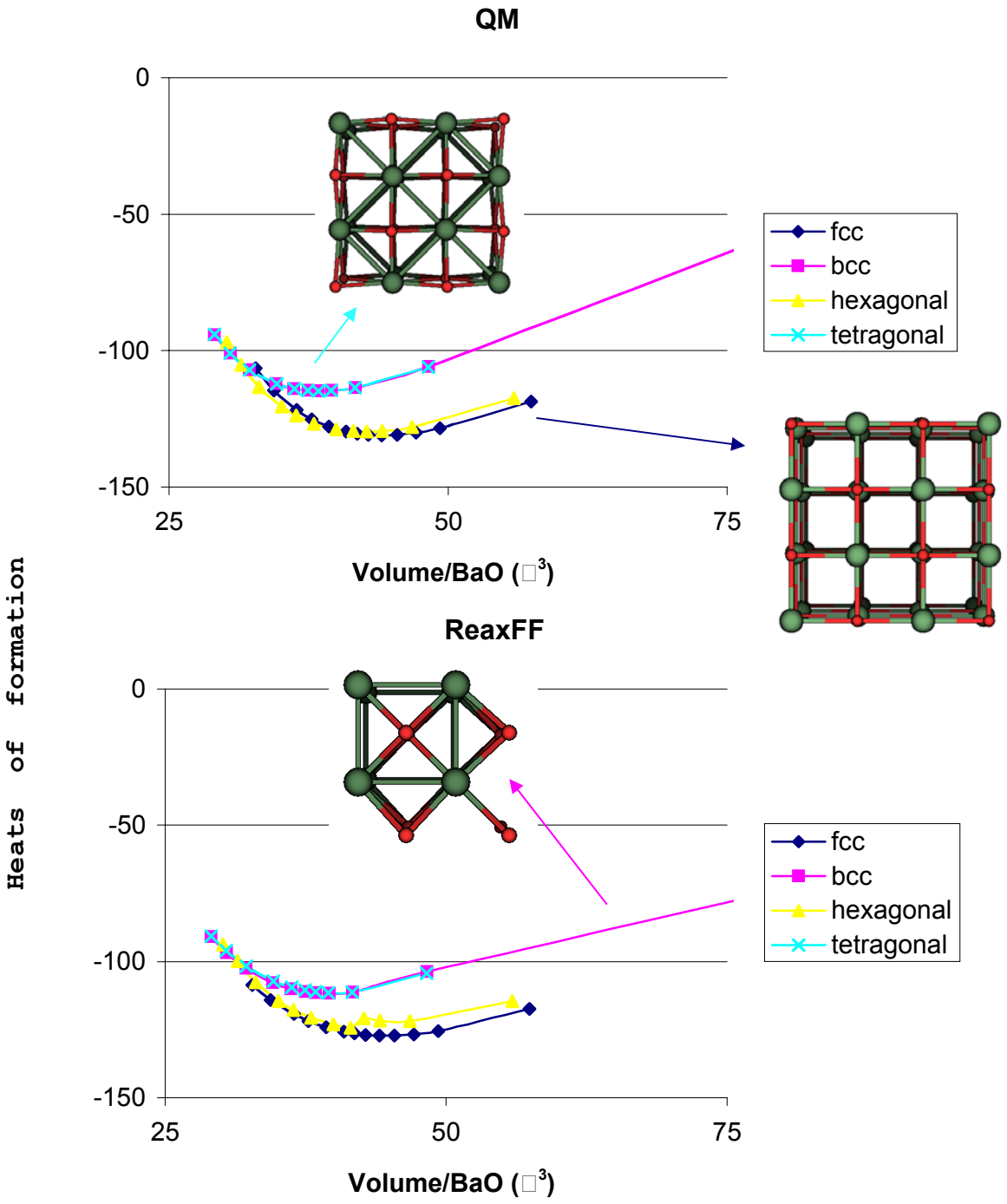

Fig.7. QM- and ReaxFF results for the equations of state of various BaO polymorphs.

Y-doped $BaZrO_3$. In our development of initial ReaxFF potentials for Y-doped $BaZrO_3$ the main focus was to reproduce the QM relative energies and geometries for various structural configurations of $BaY_xZr_{1-x}H_xO_3$, in which the hydrogen atoms occupied different possible positions. As one can see from Fig.8, we obtained really good agreement between the QM and ReaxFF data.

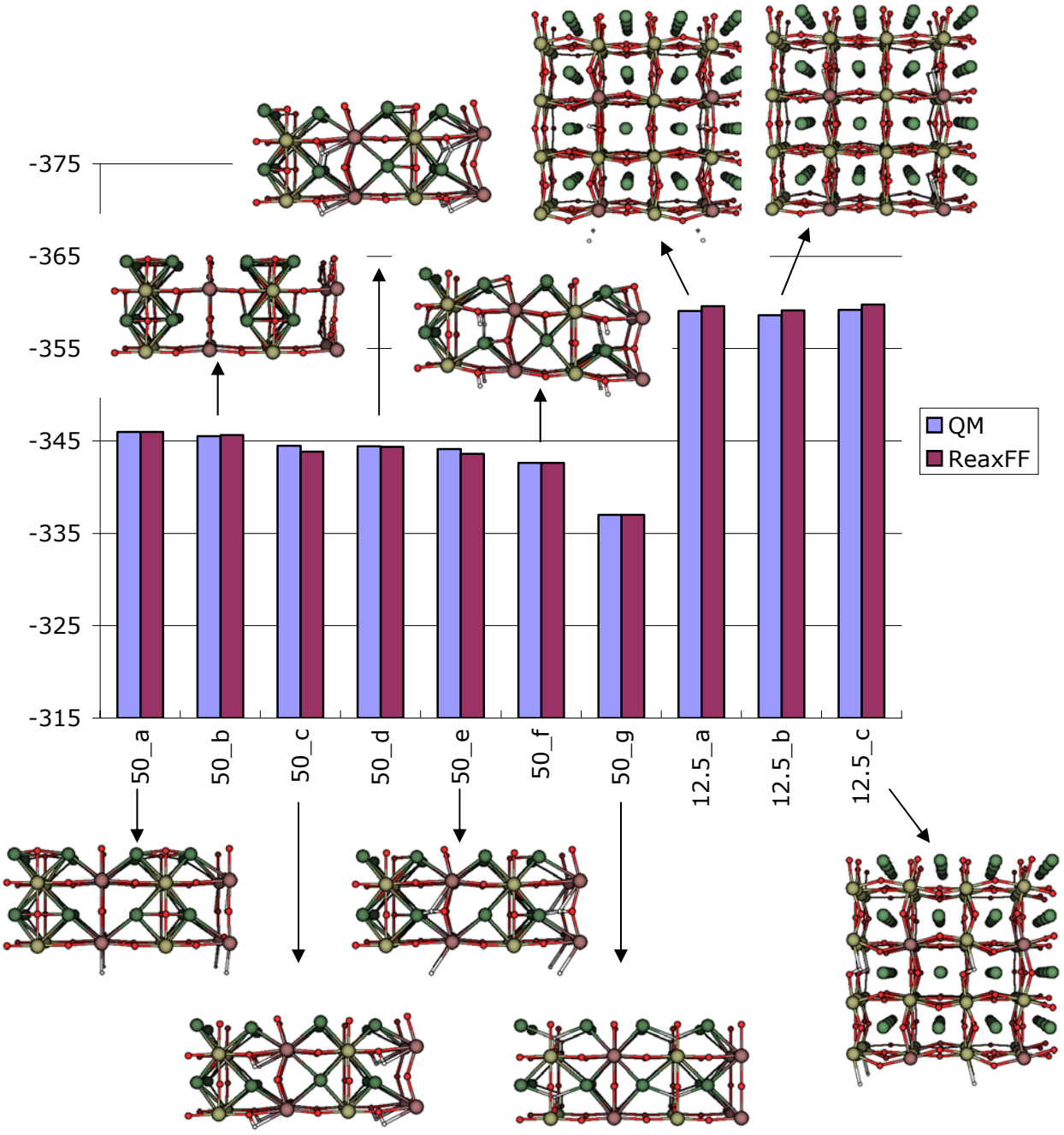

Fig.8. Heats of formation (in kcal/mol) for Y-doped (50% and 12.5% mol) $BaZrO_3$-phases.

EXPERIMENTAL

Process for dense Y-doped $BaZrO_3$

As reported in literature, it is difficult to readily process $BaZrO_3$ to a high density (>93%). Usually extreme conditions, such as high temperature (1700-1800°C), long sintering times (24 h), and nanometer particle size are needed to prepare a fully densified pellet. Well-densified electrolyte is crucial for electrochemical cells because it allows for the separation of the reactants. High temperature sintering to attain a dense sample is not practical for the development of thin-film supported electrolyte due to the fact that the cell components (electrolyte and support) need to be co-sintered. Decreasing the sintering temperature will (i) allow for a wider range of materials to be used for the support, (ii) assist in better matching of thermal expansion of the components, and (iii) avoid the loss of barium, which has been previously reported to occur at high temperatures.

To accelerate the densification process at lower temperature, sintering aids were utilized. An initial screening of all transition elements in the series Sc to Zn, showed NiO, CuO and ZnO to be the most effective additives for enhancing barium zirconate densification, as shown in Fig.9. As evident from the data, Ni, Cu, and Zn enhanced densification from about 60% of theoretical for the unmodified material to approximately 86-88% for modified BYZ, which later is improved to 95% with refined mixing techniques, Fig.10. Other additives such as V, Cr and Fe, in contrast, substantially worsened densification behavior. Diffraction patterns after sintering for Ni, Cu, and Zn are presented in Fig.11 and all confirm a single perovskite phase. Upon closer examination under SEM (Fig.12) equipped with EDS the Cu modified sample showed the presence of $Ba_2YCu_3O_x$ phase. Due to the presence of the second phase, Cu was eliminated as a modifier. The Ni modified BYZ pellets changed color to black after sintering, while the Zn modified changed to a light green. A color change from white to black usually suggests the presence of electronic conductivity. However, it should be noted that a minimal amount of transitional metal oxide was added, which is unlikely to significantly increase electronic conduction in the sample. Since Ni and Zn produce similar results and to be cautious of electronic conductivity, Zn was chosen as the best modifier.

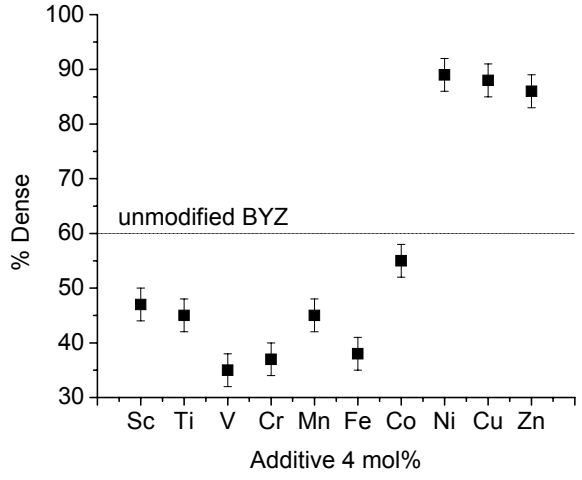

Fig.9. Effect of transitional metal oxide additives as sintering aids for BYZ.

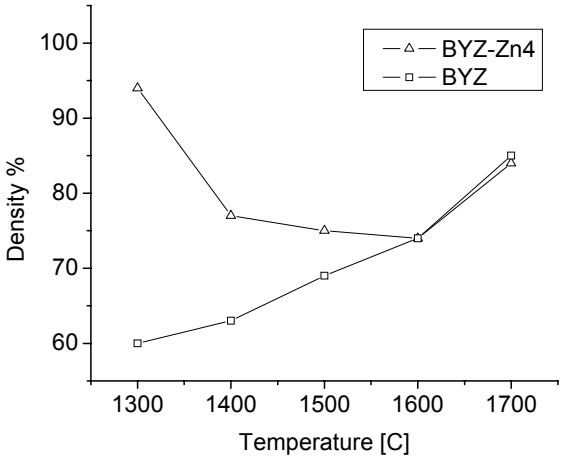

Fig.10. Density of BYZ and BYZ-Zn4 as a function of sintering temperature in air.

The difference in sintering behavior between unmodified and Zn-modified BYZ is particularly evident from a comparison of densities as a function of temperature, Fig.10. For BYZ-Zn4, the density reached 95% of theoretical value D_t (D_t = 6.12 g/cm^3) at 1300°C compared to the maximum density of 88% for BYZ at 1700°C. Microstructure of the Zn-modified BYZ is highlighted in Fig.13. As can be seen, a dense surface was achieved with a homogenous grain size distribution and average grain size of 1 μm.

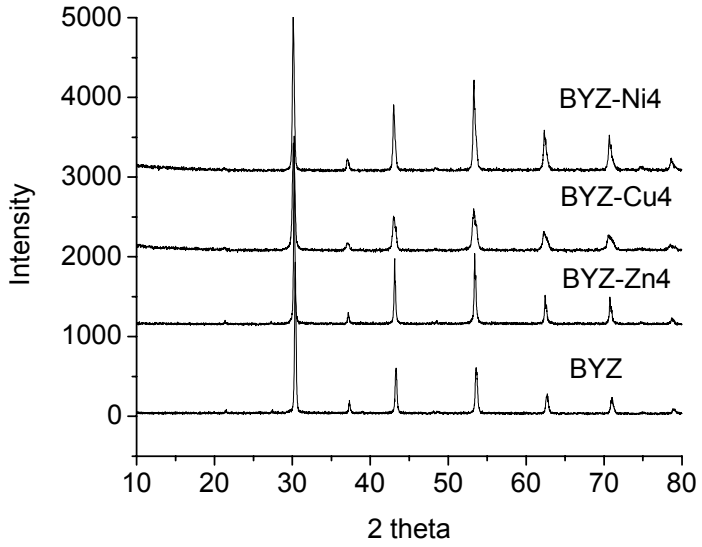

Fig.11. X-ray powder diffraction patterns of sintered BYZ, BYZ-Zn4, BYZ-Cu4, and BYZ-Ni4.

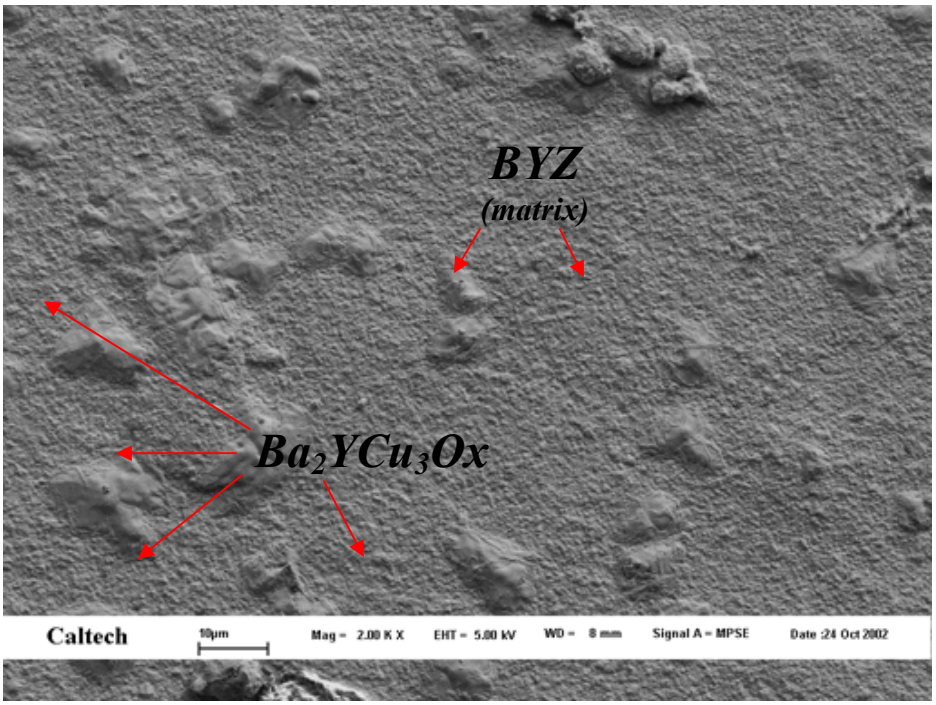

Fig.12. Surface of sintered (1300C) BYZ-Cu4 pellet.

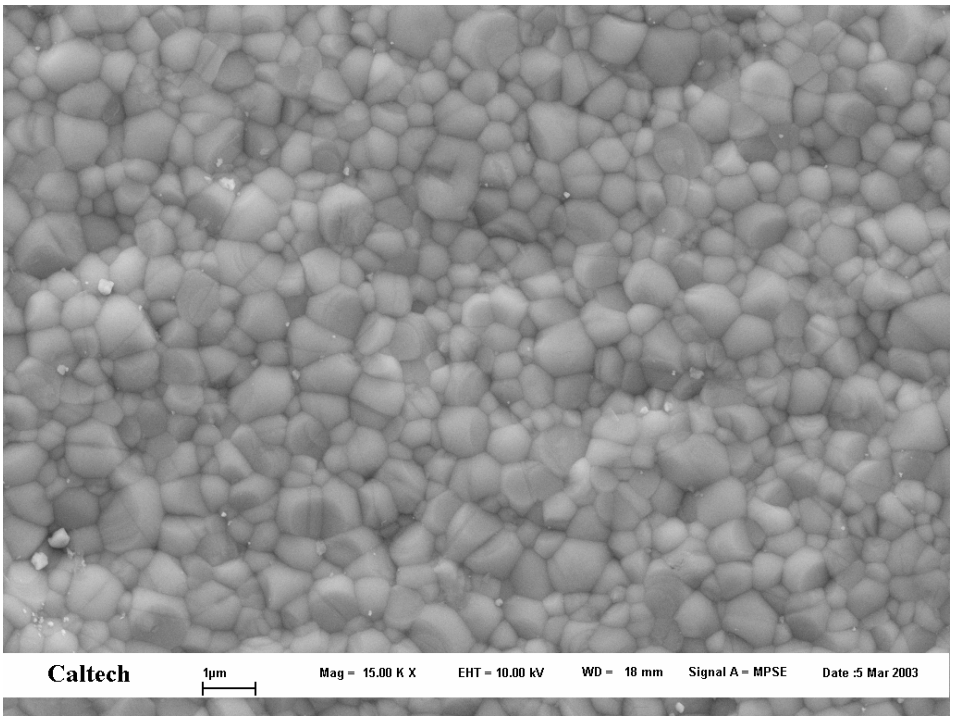

Fig.13. SEM surface micrograph of sintered BYZ-Zn4 at 1300C.

The temperature dependence of the bulk conductivity σ_{gi}, grain boundary conductivity σ_{gb}, and specific grain boundary conductivity $\sigma_{sp.gb}$ are presented in Fig.14a for BYZ-Zn4 and in Fig.14b for BYZ. The bulk conductivity of BYZ agrees with the highest reported value [7], shown in the Fig.14. Bulk conductivity of the BYZ-Zn4 is slightly lower than that of unmodified BYZ. The lower bulk conductivity of the BYZ-Zn4 system can be attributed to the lower pre-exponential factor. This suggests that the concentration of charge carriers is lower in the bulk of BYZ-Zn4. It can be seen that for the BYZ system with an average grain size of 1 μm, the total conductivity is dominated by the grain boundary until approximately 590°C, at which the total grain boundary and bulk conductivities intercept. To successfully operate in the temperature region of 400-500°C with a maximum conductivity, a microstructure with approximately 3 μm is needed. This will move the interception of the total grain boundary and the bulk conductivity to ~390°C.

Table 1. Comparison of activation energies and pre-exponential factor of bulk and grain boundary conductivity of BYZ-Zn4 and BYZ.

Bulk	BYZ-Zn4	BYZ
E_a, gi [eV]	0.47	0.44
Log A, gi	3.505	3.696
Boundary		
E_a, gb [eV]	0.71	0.69
Log A, gb	5.412	5.138

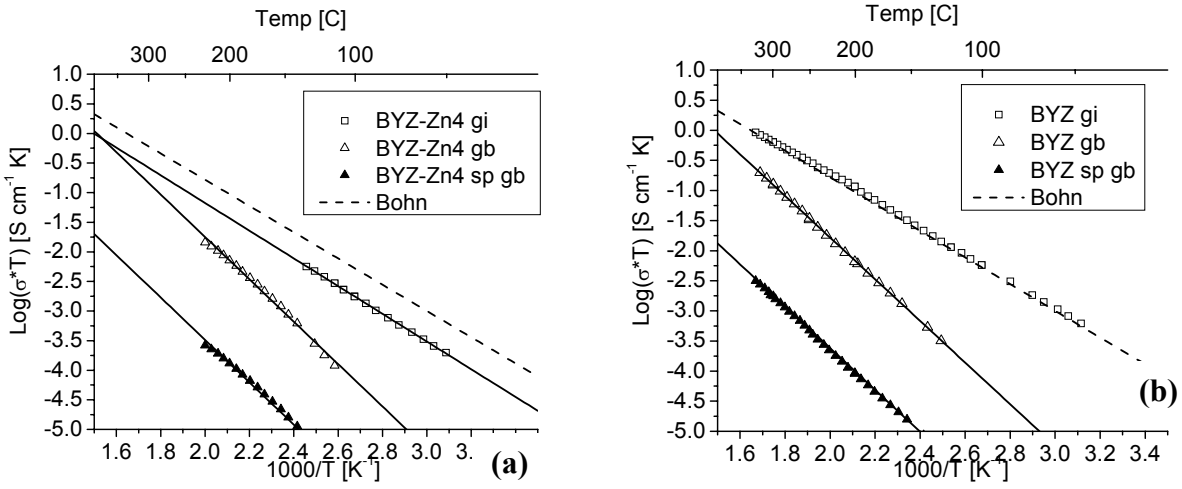

Fig.14. The bulk, total grain boundary, and specific grain boundary conductivity of BYZ-Zn4 (a) and of BYZ (b) as a function of temperature plotted in Arrhenius form. Atmosphere is water-saturated nitrogen.

CONCLUSIONS

A series of QM calculations of EOS has been performed on various bulk metals (Zr, Y, Ba), metal alloys (Y/Zr), and metal oxides (ZrO_2, Y_2O_3, BaO). The obtained QM data were then used to optimize ReaxFF parameters.

We currently have the ReaxFF description for Pt-metal clusters, various bulk metals (Pt, Zr, Y, Ba), metal alloys (Y/Zr), metal oxides (ZrO_2, Y_2O_3, BaO) and initial ReaxFF potentials for Y-doped $BaZrO_3$.

To accelerate the densification process of $BaZrO_3$ ceramics at lower temperature, an initial screening of all transition elements in the series Sc to Zn has been performed. It turned out that NiO, CuO and ZnO are the most effective additives for enhancing barium zirconate densification. The enhanced densification for modified BYZ has been improved to 95% with refined mixing techniques.

Characterization (X-ray diffraction, scanning electron microscopy, and impedance spectroscopy) of Zn-, Cu- and Ni-modified BYZ has been performed. The temperature dependence of the bulk conductivity σ_{gi}, grain boundary conductivity σ_{gb}, and specific grain boundary conductivity $\sigma_{sp.gb}$ were measured. The bulk conductivity of BYZ-Zn4 is slightly lower than that of unmodified BYZ.

For the BYZ system with an average grain size of 1 μm, the total conductivity is dominated by the grain boundary until approximately 590C, at which the total grain boundary and bulk conductivities intercept.

To successfully operate in the temperature region of 400-500C with a maximum conductivity, a microstructure with approximately 3 μm is needed. This will move the interception of the total grain boundary and the bulk conductivity to ~390C.

In the forthcoming months the following investigations will be performed:

We will continue developing ReaxFF based on the interaction between QM and ReaxFF results. Diffusion barriers will be added to the training set which will allow us to perform MD simulations of diffusion processes in the Y-doped $BaZrO_3$ electrolyte and electrode/electrolyte interface.

QM calculations on stable $BaZrO_3$ surfaces will be performed for further modeling grain boundaries. We will start applying ReaxFF on the realistic electrolyte structures to study proton transport in BYZ grains and grain boundaries.

Potential cathode materials (transition metal perovskite) will be screened for reactivity with BYZ.

Total conductivity of viable cathode materials will be measured for further screening.

Optimal cathode catalyst in terms of reactivity and conductivity will be identified.

REFERENCES

1. K.D. Kreuer, St. Adams, W. Munch, A. Fuchs, U.Klock, J. Maier, *Solid State Ionics* **145** 295 (2001).
2. A. C. T. van Duin, S. Dasgupta, F. Lorant, and W. A. Goddard, *J. Phys. Chem.* **A105** 9396 (2001).
3. A. C. T. van Duin, A. Strachan, S. Stewman, Q. Zhang, X. Xu, and W. A. Goddard, *J. Phys. Chem.* **A107** 3803 (2003).
4. P.Hohenberg and W.Kohn*, Phys. Rev*. **136** 864B (1964).
5. W.Kohn and L. J. Sham, *Phys. Rev*. **140** 1133A (1965).
6. J. P. Perdew, K.Burke and M. Ernzerhof, *Phys. Rev. Lett. 77* 3865 (1996).
7. H.G. Bohn and T. Schober, *J. Am. Ceram. Soc.* **83** 768 (2000).

LIST OF ACRONYMS AND ABBREVIATIONS

BYZ - $BaZr_{1-x}Y_xO_{3-\delta}$

DFT - Density Functional Theory,

EOS - Equation of States,

GGA - Generalized Gradient Approximation,

MD - Molecular Dynamics,

PC SOFC – Proton Conducting Solid Oxide Fuel Cell,

QM - Quantum Mechanics,

ReaxFF - First Principles-Based Reactive Force Fields,

SEM – Scanning Electron Microscopy

XRD – X-ray Diffraction